PHYSICAL REVIEW B **93**, 075124 (2016)

Interplay between spin-density wave and 3*d* local moments with random exchange in a molecular conductor

Genta Kawaguchi,[1] Mitsuhiko Maesato,[1,*] Tokutaro Komatsu,[1] Tatsuro Imakubo,[2] and Hiroshi Kitagawa[1]
[1]*Division of Chemistry, Graduate School of Science, Kyoto University, Kitashirakawa-Oiwakecho, Sakyo-ku, Kyoto 606-8502, Japan*
[2]*Department of Materials Science and Technology, Nagaoka University of Technology, 1603-1 Kamitomioka, Nagaoka, Niigata 940-2188, Japan*

(Received 25 November 2015; published 11 February 2016)

We present the results of high-pressure transport measurements on the anion-mixed molecular conductors $(\mathrm{DIETSe})_2M\mathrm{Br}_2\mathrm{Cl}_2$ [DIETSe = diiodo(ethylenedithio)tetraselenafulvalene; M = Fe, Ga]. They undergo a metal-insulator (M-I) transition below 9 K at ambient pressure, which is suppressed by applying pressure, indicating a spin-density-wave (SDW) transition caused by a nesting instability of the quasi-one-dimensional (Q1D) Fermi surface, as observed in the parent compounds $(\mathrm{DIETSe})_2M\mathrm{Cl}_4$ (M = Fe, Ga). In the metallic state, the existence of the Q1D Fermi surface is confirmed by observing the Lebed resonance. The critical pressures of the SDW, P_c, of the $M\mathrm{Br}_2\mathrm{Cl}_2$ (M = Fe, Ga) salts are significantly lower than those of the the $M\mathrm{Cl}_4$ (M = Fe, Ga) salts, suggesting chemical pressure effects. Above P_c, field-induced SDW transitions appear, as evidenced by kink structures in the magnetoresistance (MR) in both salts. The $\mathrm{FeBr}_2\mathrm{Cl}_2$ salt also shows antiferromagnetic (AF) ordering of *d* spins at 4 K, below which significant spin-charge coupling is observed. A large positive MR change up to 150% appears above the spin-flop field at high pressure. At low pressure, in particular below P_c, a dip or kink structure appears in MR at the spin-flop field, which shows unconventionally large hysteresis at low temperature ($T < 1$ K). The hysteresis region clearly decreases with increasing pressure towards P_c, strongly indicating that the coexisting SDW plays an important role in the enhancement of magnetic hysteresis besides the random exchange interaction.

DOI: 10.1103/PhysRevB.93.075124

I. INTRODUCTION

Coupling between the spin and charge degrees of freedom is a major issue in solid state physics, because it involves a variety of physical phenomena including giant magnetoresistance (GMR) [1,2] and unconventional superconductivity [3–5]. One of the fascinating playgrounds for spin-charge interactions is the family of π-d hybrid molecular conductors [6–11], where the strongly correlated π electrons and local magnetic moments of d-electron spins coexist and mutually interact.

Among the π-d conductors, we focus on the quasi-one-dimensional (Q1D) systems with spin-density-wave (SDW) instability. The SDW is a symmetry-broken ground state caused by electron-electron correlation, associated with a spatially periodic modulation of spin density. It is considered that the SDW instability of π electrons can couple to periodic local moments of d spins in Q1D π-d systems. Indeed, some Q1D π-d conductors exhibit anomalous magnetoresistance (MR) associated with reconfiguration of antiferromagnetic (AF) d spins, indicating the interplay between the local moments and itinerant electrons [12–21].

The coexistence of the SDW and 3d local moments has been studied in $(\mathrm{DIETSe})_2\mathrm{FeCl}_4$, where DIETSe represents diiodo(ethylenedithio)tetraselenafulvalene [Fig. 1(a)] [17–19]. The $(\mathrm{DIETSe})_2M\mathrm{Cl}_4$ (M = Fe, Ga) compounds undergo a metal-insulator (M-I) transition at about 12 K as a result of the nesting instability of Q1D Fermi surfaces. A ^{77}Se nuclear magnetic resonance (NMR) study confirmed the onset of an incommensurate SDW (ICSDW) in the GaCl_4 salt without d spins ($S = 0$) [22]. The FeCl_4 salt also shows an AF order of d spins below 2.5 K. The coexistence of an ICSDW of π electrons and the AF order of d spins gives rise to anomalous spin-charge-coupled phenomena such as spin-flop switching and memory [18,19].

The nesting instability of Q1D Fermi surfaces can be suppressed by substituting Cl with Br. $(\mathrm{DIETSe})_2\mathrm{GaBr}_4$ shows normal metallic behavior down to 2 K, whereas $(\mathrm{DIETSe})_2\mathrm{FeBr}_4$ undergoes an M-I transition induced by AF ordering of d spins at 7 K [17,21]. It suggests that the Ruderman-Kittel-Kasuya-Yosida (RKKY)-type interaction [23–25] with the SDW instability plays an important role in the FeBr_4 salt. The higher Néel temperature T_N of the FeBr_4 salt indicates stronger π-d interactions than in the FeCl_4 salt. In fact, the FeBr_4 salt exhibits a very large hysteresis loop in MR on the order of 20 T, associated with AF ordering [20].

In order to finely control the electronic states and explore novel spin-charge-coupled phenomena, we have developed anion-mixed salts $(\mathrm{DIETSe})_2M\mathrm{Br}_2\mathrm{Cl}_2$ (M = Fe, Ga) [21]. The $M\mathrm{Br}_2\mathrm{Cl}_2$ (M = Fe, Ga) salts are isostructural with the parent MX_4 (M = Fe, Ga; X = Br, Cl) salts [Fig. 1(b)], having similar Q1D Fermi surfaces with nesting instability [Fig. 1(c)]. The $M\mathrm{Br}_2\mathrm{Cl}_2$ (M = Fe, Ga) salts exhibit an M-I transition below 9 K, indicative of the ICSDW transition. In addition, an AF transition of d spins takes place at about 4 K in the $\mathrm{FeBr}_2\mathrm{Cl}_2$ salt. These results indicate that the $M\mathrm{Br}_2\mathrm{Cl}_2$ (M = Fe, Ga) salts have almost intermediate dimensionality of π electrons and π-d interactions between the $M\mathrm{Cl}_4$ and $M\mathrm{Br}_4$ (M = Fe, Ga) salts.

Remarkably, we observed a large shift in the spin-flop field of d spins at low temperatures below about 1.3 K in $(\mathrm{DIETSe})_2\mathrm{FeBr}_2\mathrm{Cl}_2$, which resulted in large hysteresis in both MR and magnetization [21]. On the other hand, in the pristine $\mathrm{Fe}X_4$ (X = Br, Cl) salts, the hysteresis of the

---

[*] Corresponding author: maesato@kuchem.kyoto-u.ac.jp

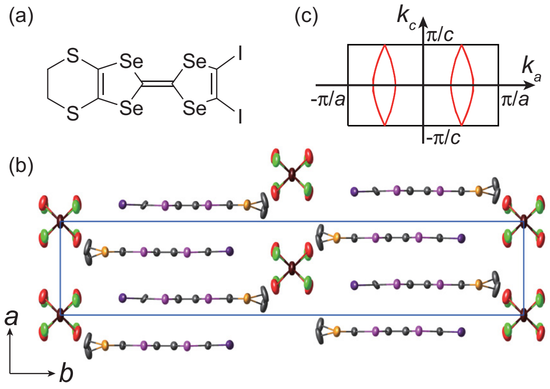

FIG. 1. (a) Molecular structure of DIETSe. (b) Crystal structure of $(DIETSe)_2FeBr_2Cl_2$ viewed from the c axis (C, gray; I, violet; Se, pink; S, yellow; Fe, brown; Br, red; and Cl, green). DIETSe molecules only in the plane $c = 1/2$ are indicated. (c) Fermi surfaces of $(DIETSe)_2FeBr_2Cl_2$ calculated by density-functional theory (DFT) [21].

spin-flop field is negligibly small [18–21]. These differences are attributable in part to the random exchange in the $FeBr_2Cl_2$ salt. The randomly substituted halogens in magnetic anions give rise to locally different exchange fields, leading to the hysteretic response to the external magnetic field. The inorganic magnetic alloys $K_2Fe(Br_xCl_{1-x})_5H_2O$ ($x = 0.1, 0.2, 0.3$) exhibited similar hysteresis, which has been explained by random exchange interactions between magnetic species [26]. However, in $(DIETSe)_2FeBr_2Cl_2$, the exchange interactions between d spins are primarily dominated by RKKY-type π-d interactions rather than direct interactions, because of the short donor-anion contacts and the long inter-anion distance [17,21], which is a peculiarity of $(DIETSe)_2FeBr_2Cl_2$. In addition, the ground state of itinerant π electrons is a SDW, which may play an important role in the emergence of a wide hysteresis.

To clarify the possible effects of the SDW on the magnetic hysteresis and explore spin-charge-coupled phenomena, we performed detailed magnetotransport studies of $(DIETSe)_2FeBr_2Cl_2$ under high pressures, because the SDW can be suppressed by pressure in a systematic manner. It is found that the hysteresis of the $FeBr_2Cl_2$ salt shows a nontrivial dependence on pressure.

II. EXPERIMENT

Single crystals of $(DIETSe)_2MBr_2Cl_2$ ($M =$ Fe, Ga) were synthesized by the electrochemical method using the same molar amount of TBA-MCl$_4$ and TBA-MBr$_4$ (TBA = tetra-n-butylammonium; $M =$ Fe, Ga) as supporting electrolytes [21]. The electrical resistivity was measured along the b axis using the four-probe method. Four gold wires (10 μm in diameter) were attached to the crystals with carbon paste. Hydrostatic pressure was applied to the samples using clamp-type BeCu pressure cells. Daphne 7373 oil was used as the pressure medium. Low-temperature pressures were determined by the pressure dependence of the superconducting transition temperature of tin. The longitudinal MR was measured under the magnetic field parallel to the b axis up to 12 T using a solenoid-type superconducting magnet. The angular-dependent MR of the $FeBr_2Cl_2$ salt was measured by rotating a small pressure cell with a single-axis rotator.

III. RESULTS AND DISCUSSION

A. Resistivity and the *P*-*T* phase diagram

The temperature dependence of the b-axis resistivity ρ_b, corresponding to interlayer resistivity, of $(DIETSe)_2MBr_2Cl_2$ ($M =$ Fe, Ga) under various pressures is shown in Figs. 2(a) and 2(b). At ambient pressure, the $GaBr_2Cl_2$ and $FeBr_2Cl_2$ salts undergo an M-I transition at 9 and 8 K, respectively. These transition temperatures are lower than those of the $GaCl_4$ and $FeCl_4$ salts. The application of pressure gradually suppressed the M-I transition in both salts. Since these behaviors are similar to those of the MCl$_4$ ($M =$ Fe, Ga) salts [18,19], the M-I transitions of the MBr_2Cl_2 ($M =$ Fe, Ga) salts are attributed to the ICSDW transitions owing to the nesting instability of Q1D Fermi surfaces with electron-electron correlation.

The $FeBr_2Cl_2$ salt also exhibits an AF transition of d spins at $T_N = 4$ K, which is confirmed by the magnetic susceptibility measurement [21]. The resistivity shows a steep increase at T_N, indicating π-d interactions [Fig. 2(b)]. In the $GaBr_2Cl_2$ salt, the ICSDW phase is totally suppressed above 3.5 kbar, and normal metallic behavior is observed down to the lowest temperature in the experiments. On the other hand, in the $FeBr_2Cl_2$ salt, while the ICSDW phase is suppressed, the steep

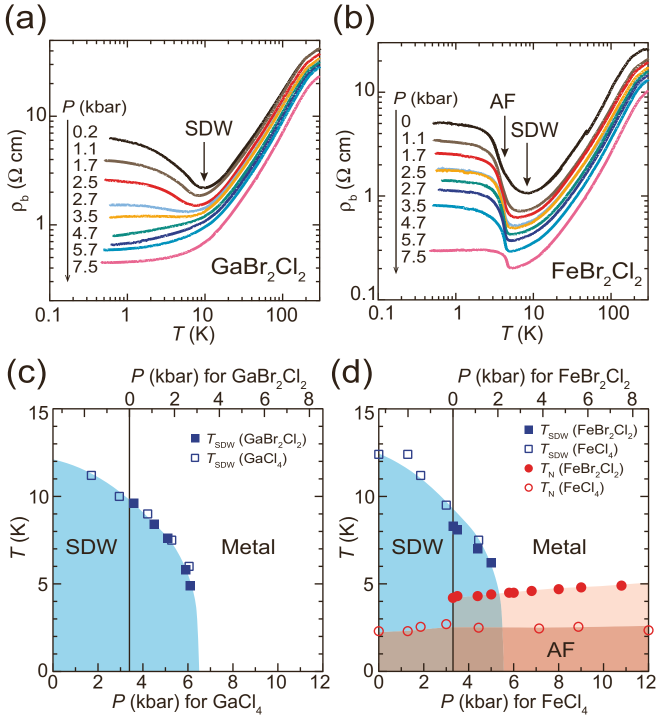

FIG. 2. The temperature dependence of the b-axis resistivity of the $GaBr_2Cl_2$ salt (a) and the $FeBr_2Cl_2$ salt (b). Pressure-temperature (P-T) phase diagrams of the $GaBr_2Cl_2$ salt (c) and the $FeBr_2Cl_2$ salt (d). P-T phase diagrams of the parent compounds, the $GaCl_4$ and $FeCl_4$ salts [18] can be collapsed into the identical phase diagrams, indicating chemical pressure effects. The upper and lower axes in the P-T phase diagrams represent the pressure for the MBr_2Cl_2 and MCl$_4$ ($M =$ Fe, Ga) salts, respectively.

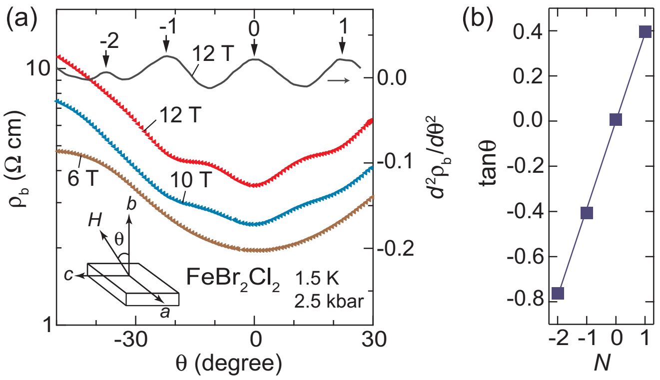

FIG. 3. (a) The angle-dependent magnetoresistance (MR) of the $FeBr_2Cl_2$ salt at 1.5 K and 2.5 kbar. The left and right axes indicate the *b*-axis resistivity ρ_b and the second-order differential of the resistivity $d^2\rho_b/d\theta^2$, respectively. The inset shows the magnetic-field angle versus the crystallographic axes. (b) The positions of the MR minimums (peaks of $d^2\rho_b/d\theta^2$) plotted against $\tan\theta$.

increase in resistance at T_N is maintained under high pressure. It is attributed to an AF order-induced M-I transition [17–21].

The pressure-temperature (P-T) phase diagrams of the $GaBr_2Cl_2$ and $FeBr_2Cl_2$ salts are shown in Figs. 2(c) and 2(d), respectively, as well as those of the $GaCl_4$ and $FeCl_4$ salts [18]. The SDW critical pressures P_c of the $GaBr_2Cl_2$ and $FeBr_2Cl_2$ salts are about 3.1 and 2.2 kbar, respectively. The present results are well merged into the P-T phase diagrams of the $GaCl_4$ and $FeCl_4$ salts by simply adjusting P_c. These results indicate that the 50% Br substitution corresponds to chemical pressure of about 3.3 kbar.

B. Angle-dependent magnetoresistance

To investigate the topology of the Fermi surface and the effect of AF ordering of *d* spins, angular-dependent MR measurements were performed. Figure 3(a) shows the angle dependence of MR in the $FeBr_2Cl_2$ salt at 1.5 K under 2.5 kbar just above P_c (= 2.2 kbar), where the resistivity is measured along the *b* axis. The low-temperature pressure was estimated by considering the pressure loss during cooling [27], because the pressure cell for the angle-dependent measurement was too small to include the tin manometer. As shown in the inset drawing, the magnetic field was rotated in the *bc* plane, which is perpendicular to the most conducting *a*-axis direction. The angle θ was measured from the *b* axis. At high magnetic fields above 8 T, MR shows local minima at fixed angles, as shown by the peak in the second derivative of resistivity $d^2\rho_b/d\theta^2$ at 12 T. The MR minimum appears at magic angles, which follow $\tan\theta = 0.39N$ ($N = 0, \pm1, \pm2,\ldots$), as shown in Fig. 3(b). It indicates the Lebed resonance of Q1D Fermi surfaces satisfying the condition

$$\tan\theta = \frac{c}{b} \times N,$$

where *c* and *b* are lattice constants normal to the most conductive direction [28–32]. The ratio c/b of the $FeBr_2Cl_2$ salt is 0.374 at 293 K [21], which is comparable to the observed coefficient of 0.39. This confirms the existence of Q1D Fermi surfaces above P_c and 8 T in the $FeBr_2Cl_2$ salt. On the other hand, the Lebed resonance disappears at 6 T in the $FeBr_2Cl_2$ salt, suggesting reconstruction of the Q1D Fermi surfaces by AF ordering of *d* spins at 6 T.

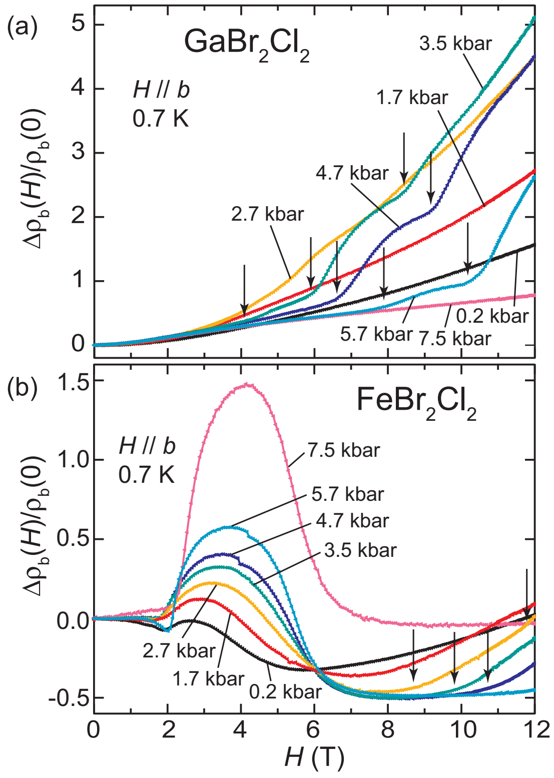

FIG. 4. Interlayer MR of the $GaBr_2Cl_2$ salt (a) and the $FeBr_2Cl_2$ salt (b) at 0.7 K and at various pressures under a magnetic field along the *b* axis. For comparison, the MR change is normalized by the value at 0 T. Arrows represent the onsets of the FISDW transitions.

C. Field-induced transitions and mutual π-d interactions

Figures 4(a) and 4(b) show the interlayer MR of the $GaBr_2Cl_2$ and $FeBr_2Cl_2$ salts, respectively, at 0.7 K and various pressures. The magnetic field and current are applied along the least conducting *b*-axis direction. At low pressures, the $GaBr_2Cl_2$ salt shows a monotonic increase in MR because of the SDW ground state. At high pressures above P_c (= 3.1 kbar), we found a series of steplike steep increases in MR with kink structures as indicated by arrows. The kink fields shift to higher magnetic fields with increasing pressure and exceed 12 T at 7.5 kbar. At the same pressure, the kink and MR increase are more pronounced at lower temperature, as shown in Fig. 5(a), which indicates the results at 3.5 kbar. These behaviors are attributable to field-induced SDW (FISDW) transitions observed in Q1D organic conductors such as $(TMTSF)_2X$ (TMTSF = tetramethyltetraselenafulvalene; X = PF_6, ClO_4, etc.) [33] and $(DIETSe)_2MCl_4$ (M = Fe, Ga) [19]. We also find FISDW transitions in the $FeBr_2Cl_2$ salt at a high magnetic field [Figs. 4(b) and 5(b)], although they are less pronounced. To the best of our knowledge, $(DIETSe)_2FeBr_2Cl_2$ is the second example of a compound showing both AF and FISDW phases after $(DIETSe)_2FeCl_4$ [19].

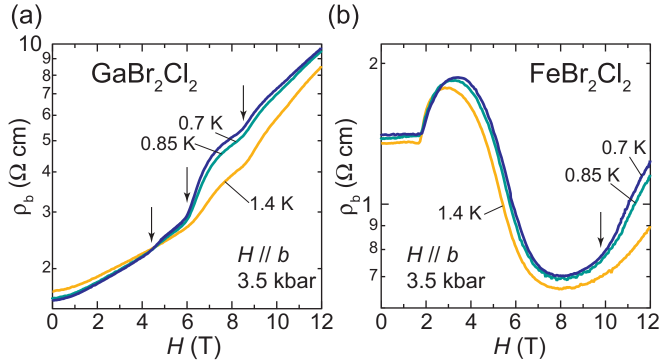

FIG. 5. Interlayer MR of the GaBr$_2$Cl$_2$ salt (a) and the FeBr$_2$Cl$_2$ salt (b) at 3.5 kbar and 0.7, 0.85, 1.4 K under a magnetic field along the b axis. Arrows represent the onsets of the FISDW transitions. The resistivity is shown in logarithmic scale.

Furthermore, the FeBr$_2$Cl$_2$ salt exhibits anomalous MR at low magnetic fields below 7 T, unseen in the GaBr$_2$Cl$_2$ salt. The dip structures or steep increases in MR around 2 T are attributed to spin-flop transition of d spins as confirmed by magnetic measurements [21]. The MR change, $\Delta\rho_b(H)/\rho_b(0) = [\rho_b(H) - \rho_b(0)]/\rho_b(0)$, above the spin-flop field increases with increasing pressure, reaching as large as 150% at 7.5 kbar. The large anomalies in MR are suppressed above about 7 T, which corresponds to the boundary of the AF phase as confirmed by the magnetic torque measurements [21]. These behaviors of the MR are similar to those of the MCl$_4$ (M = Fe, Ga) salts [18,19]. However, the hysteresis around the spin-flop field is significantly different between the FeBr$_2$Cl$_2$ and FeCl$_4$ salts, as discussed below.

The up- and down-sweep MR of (DIETSe)$_2$FeBr$_2$Cl$_2$ at various temperatures under ambient pressure are shown in Fig. 6(a) [21]. Below about 1.3 K, the MR shows a large hysteresis involving shift of the dip position, indicating hysteresis of the spin-flop field. The hysteresis becomes more pronounced with decreasing temperature. We also confirmed the emergence of magnetic hysteresis associated with the spin-flop transition below about 1.3 K by superconducting quantum interference device (SQUID) measurements using a ^{3}He cryostat [21]. Meanwhile, the parent FeCl$_4$ salt shows negligibly small magnetic hysteresis at the spin-flop transition [18,21], despite the irreversible hysteresis in conductivity [18]. These results strongly suggest the importance of the random exchange interactions caused by anion mixing in the FeBr$_2$Cl$_2$ salt.

Figures 6(b), 6(c), and 6(d) display the MR at 1.7, 3.5, and 7.5 kbar, respectively. The MR also shows hysteresis under pressure. The hysteresis of the spin-flop field tends to decrease with increasing pressure. At high pressures, the difference between the up- and down-sweep MR becomes significant just below the AF boundary [Figs. 6(c) and 6(d)].

Figure 6(e) shows the magnetic-field–temperature (H-T) phase diagrams for 0, 1.7, 3.5, and 7.5 kbar. At low pressure, where the SDW phase (colored blue) exists, a wide hysteresis region is observed as shown in the brown area. The hysteresis region clearly decreases with increasing pressure from 0 to 3.5 kbar, and is nearly unchanged above P_c. This behavior strongly suggests that the spin-flop hysteresis is reinforced by the SDW of π electrons.

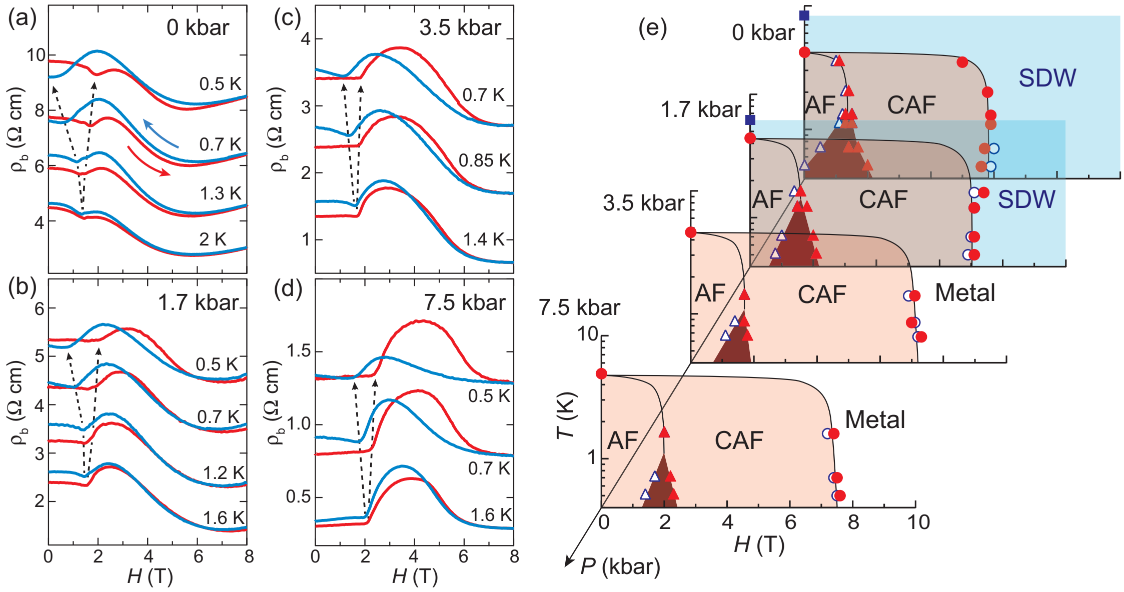

FIG. 6. MR hysteresis in the FeBr$_2$Cl$_2$ salt at various temperatures under pressures of 0 kbar [21] (a), 1.7 kbar (b), 3.5 kbar (c), and 7.5 kbar (d). The red and light-blue curves indicate up and down sweeps, respectively. Broken arrows show the shift of the MR dip structure. The data for (b)–(d) are collected up to 12 T and shown up to 8 T here. Some data are shifted vertically for clarity. (e) Magnetic-field–temperature (H-T) phase diagrams of the FeBr$_2$Cl$_2$ salt at 0, 1.7, 3.5, and 7.5 kbar. The temperature axis is shown from 0.4 to 10 K in logarithmic scale. Blue squares indicate the ICSDW transition temperatures at 0 T. Red and open blue circles denote the offsets of positive MR on the up and down sweeps, respectively, suggesting the AF phase boundary. Red and open blue triangles represent dip structures of the up- and down-sweep MR, respectively, corresponding to the spin-flop field. Regions painted blue, pink, and brown indicate the ICSDW phase, the AF phase, and the hysteresis of the spin-flop field, respectively.

Above P_c, the transition between AF and the paramagnetic (PM) phases is associated with the M-I transition. The field-induced AF-PM transition manifests a first-order nature at low temperature.

The magnetic hysteresis in $(DIETSe)_2FeBr_2Cl_2$ is in part explained by random exchange interactions of d spins as discussed in inorganic magnetic alloys [26] and domain wall dynamics, particularly at high pressures above P_c. The mixing of anions introduces random exchange interactions as well as distribution of the magnetic anisotropy, which would affect the reconfigurations of magnetic moments and domain wall dynamics under an applied magnetic field to cause magnetic hysteresis. However, the hysteresis is markedly pronounced below P_c, which requires an additional mechanism.

The reconfigurations of $3d$ local moments cause scattering of itinerant electrons, which gives rise to a large change in MR. What is remarkable in the present compound is that the coexistence of the ICSDW alters the reconfigurations of $3d$ local moments, particularly at low temperatures, as seen in the hysteresis of the magnetic moments at ambient pressure [21]. It indicates a mutual interaction between ICSDW and AF moments.

The ICSDW is considered to be pinned by impurities, lattice defects, and random exchange potentials from magnetic anions. Otherwise, the Fröhlich collective mode would appear at zero frequency [34]. As for the excitations of the SDW condensate, phase and amplitude excitations should be taken into account. An internal deformation of the condensate would occur when interacting with pinning potentials. At low temperature, phase deformation of the SDW is more likely to occur than amplitude deformation because the latter needs larger energy. In the present system, a number of pinning centers are expected to exist because of the random halogen substitution in magnetic anions. Because the deformation of SDW around the pinning center is possible, such an effect may in turn alter the response of the $3d$ local moments against the external magnetic field due to exchange interactions.

We also note that the density waves often show glassy behaviors at low temperature [35–37]. Low-lying excitations involve the dynamics of internal deformations of a density-wave condensate, which can be screened by quasi-particles at high temperature. At low temperature, the long-time relaxation process may appear due to the deformations of condensate with many possible metastable states, leading to glassy behaviors and memory phenomena. Indeed, the SDW compound $(TMTSF)_2PF_6$ shows a low-frequency tail in the conductivity, indicating a glassy nature [38]. The pulse-sign and pulse-duration memory effects also appear in the TMTSF salts under an electric field [39,40]. However, the SDW state of the TMTSF salts is complicated because of the subphase structure and coexistence of purely electronic charge-density wave [41,42] that disappears at low temperature [43], but these are out of scope of the present paper.

In the present anion-mixed salt $(DIETSe)_2FeBr_2Cl_2$, random exchange interactions between $3d$ local moments and ICSDW might play a role in the electromagnetic dynamics. Such a system has never been reported to date. We found that the disappearance of ICSDW significantly reduces the hysteresis of the spin-flop transition. We, therefore, speculate that a synergistic effect between the glassy nature of SDW and the random exchange gives rise to the large hysteresis below P_c.

IV. CONCLUSIONS

We have investigated the effects of high pressure and high magnetic field on the electronic states in anion-mixed molecular conductors $(DIETSe)_2MBr_2Cl_2$ (M = Fe, Ga). Pressure suppresses the M-I transition attributed to ICSDW formation, which is demonstrated by the appearance of the Lebed resonance in the high-pressure metallic state. The SDW critical pressures P_c of the MBr_2Cl_2 (M = Fe, Ga) salts are reduced by ca. 3.3 kbar by half Br substitution compared with those of the MCl_4 (M = Fe, Ga) salts, indicating the chemical pressure effect. Above P_c, the MR steeply increases involving kink structures in both the MBr_2Cl_2 (M = Fe, Ga) salts, suggesting FISDW transitions.

The $FeBr_2Cl_2$ salt exhibits anomalous MR triggered by the spin-flop transition of d spins below T_N with a change $\Delta\rho_b(H)/\rho_b(0)$ up to 150%. This indicates the highly susceptible nature of low-dimensional π elections against the AF ordering of localized d spins.

Furthermore, the MR also shows hysteresis associated with a large shift in the spin-flop field at low temperature ($T < 1.3$ K). The width of the hysteresis is found to decrease considerably with increasing pressure towards P_c, but is nearly unchanged above P_c. These results demonstrate a profound influence of SDW on the reconfigurations of $3d$ local moments. We propose a synergistic effect between the glassy nature of SDW and the random exchange interaction to account for the unconventional hysteresis.

ACKNOWLEDGMENTS

This work was in part supported by Grants-in-Aid for JSPS Fellows (25-1778), Scientific Research (C) (25400367), (C) (25410090), and (S) (23225005) from JSPS, and CREST, JST. The band calculations were performed on the supercomputer of ACCMS, Kyoto University, and SuperComputer System, Institute for Chemical Research, Kyoto University.

---

[1] M. N. Baibich, J. M. Broto, A. Fert, F. Nguyen Van Dau, F. Petroff, P. Etienne, G. Creuzet, A. Friederich, and J. Chazelas, Phys. Rev. Lett. **61**, 2472 (1988).

[2] G. Binasch, P. Grünberg, F. Saurenbach, and W. Zinn, Phys. Rev. B **39**, 4828 (1989).

[3] J. M. Tranquada, B. J. Sternlieb, J. D. Axe, Y. Nakamura, and S. Uchida, Nature (London) **375**, 561 (1995).

[4] N. D. Mathur, F. M. Grosche, S. R. Julian, I. R. Walker, D. M. Freye, R. K. W. Haselwimmer, and G. G. Lonzarich, Nature (London) **394**, 39 (1998).

[5] I. I. Mazin, D. J. Singh, M. D. Johannes, and M. H. Du, Phys. Rev. Lett. **101**, 057003 (2008).
[6] E. Coronado and P. Day, Chem. Rev. **104**, 5419 (2004).
[7] T. Enoki and A. Miyazaki, Chem. Rev. **104**, 5449 (2004).
[8] H. Kobayashi, H. B. Cui, and A. Kobayashi, Chem. Rev. **104**, 5265 (2004).
[9] T. Sugimoto, H. Fujiwara, S. Noguchi, and K. Murata, Sci. Technol. Adv. Mater. **10**, 024302 (2009).
[10] N. Hanasaki, H. Tajima, M. Matsuda, T. Naito, and T. Inabe, Phys. Rev. B **62**, 5839 (2000).
[11] S. Uji, H. Shinagawa, T. Terashima, T. Yakabe, Y. Terai, M. Tokumoto, A. Kobayashi, H. Tanaka, and H. Kobayashi, Nature (London) **410**, 908 (2001).
[12] K. Enomoto, J. Yamaura, A. Miyazaki, and T. Enoki, Bull. Chem. Soc. Jpn. **76**, 945 (2003).
[13] K. Okabe, J. Yamaura, A. Miyazaki, and T. Enoki, J. Phys. Soc. Jpn. **74**, 1508 (2005).
[14] J. Nishijo, A. Miyazaki, T. Enoki, R. Watanabe, Y. Kuwatani, and M. Iyoda, Inorg. Chem. **44**, 2493 (2005).
[15] A. Miyazaki, H. Yamazaki, M. Aimatsu, T. Enoki, R. Watanabe, E. Ogura, Y. Kuwatani, and M. Iyoda, Inorg. Chem. **46**, 3353 (2007).
[16] T. Enoki, K. Okabe, and A. Miyazaki, in *Multifunctional Conducting Molecular Materials*, edited by G. Saito, F. Wudl, R. C. Haddon, K. Tanigaki, T. Enoki, H. E. Katz, and M. Maesato (RSC Publishing, Cambridge, 2007), pp. 153–160.
[17] T. Shirahata, M. Kibune, M. Maesato, T. Kawashima, G. Saito, and T. Imakubo, J. Mater. Chem. **16**, 3381 (2006).
[18] M. Maesato, T. Kawashima, Y. Furushima, G. Saito, H. Kitagawa, T. Shirahata, M. Kibune, and T. Imakubo, J. Am. Chem. Soc. **134**, 17452 (2012).
[19] M. Maesato, T. Kawashima, G. Saito, T. Shirahata, M. Kibune, and T. Imakubo, Phys. Rev. B **87**, 085117 (2013).
[20] M. Maesato, Y. Furushima, G. Saito, H. Kitagawa, T. Imakubo, A. Kiswandhi, D. Graf, and J. S. Brooks, J. Phys. Soc. Jpn. **82**, 043704 (2013).
[21] G. Kawaguchi, M. Maesato, T. Komatsu, H. Kitagawa, T. Imakubo, A. Kiswandhi, D. Graf, and J. S. Brooks, Angew. Chem. Int. Ed. **54**, 10169 (2015).
[22] C. Michioka, Y. Itoh, K. Yoshimura, Y. Furushima, M. Maesato, G. Saito, T. Shirahata, M. Kibune, and T. Imakubo, J. Phys.: Conf. Ser. **150**, 042124 (2009).
[23] M. A. Ruderman and C. Kittel, Phys. Rev. **96**, 99 (1954).
[24] T. Kasuya, Prog. Theor. Phys. **16**, 45 (1956).
[25] K. Yosida, Phys. Rev. **106**, 893 (1957).
[26] A. Paduan-Filho, C. C. Becerra, and F. Palacio, Phys. Rev. B **43**, 11107 (1991).
[27] K. Murata, H. Yoshino, H. O. Yadav, Y. Honda, and N. Shirakawa, Rev. Sci. Instrum. **68**, 2490 (1997).
[28] A. G. Lebed and P. Bak, Phys. Rev. Lett. **63**, 1315 (1989).
[29] T. Osada, A. Kawasumi, S. Kagoshima, N. Miura, and G. Saito, Phys. Rev. Lett. **66**, 1525 (1991).
[30] M. J. Naughton, O. H. Chung, M. Chaparala, X. Bu, and P. Coppens, Phys. Rev. Lett. **67**, 3712 (1991).
[31] T. Osada, S. Kagoshima, and N. Miura, Phys. Rev. B **46**, 1812 (1992).
[32] T. Osada and E. Ohmichi, J. Phys. Soc. Jpn. **75**, 051006 (2006).
[33] W. Kang, S. T. Hannahs, and P. M. Chaikin, Phys. Rev. Lett. **70**, 3091 (1993).
[34] H. Fröhlich, Proc. R. Soc. London Ser. A **223**, 296 (1954).
[35] G. Grüner, Rev. Mod. Phys. **60**, 1129 (1988).
[36] G. Grüner, Rev. Mod. Phys. **66**, 1 (1994).
[37] P. Monceau, Adv. Phys. **61**, 325 (2012).
[38] S. Donovan, Y. Kim, L. Degiorgi, and G. Grüner, J. Phys. I (France) **3**, 1493 (1993).
[39] G. Kriza, Y. Kim, and G. Mihály, Phys. Rev. B **45**, 1466 (1992).
[40] T. Yamaguchi, M. Maesato, and S. Kagoshima, J. Phys. Soc. Jpn. **65**, 3438 (1996).
[41] J. P. Pouget and S. Ravy, J. Phys. I (France) **6**, 1501 (1996).
[42] J. P. Pouget and S. Ravy, Synth. Met. **85**, 1523 (1997).
[43] S. Kagoshima, Y. Saso, M. Maesato, R. Kondo, and T. Hasegawa, Solid State Commun. **110**, 479 (1999).